20th Australasian Fluid Mechanics Conference
Perth, Australia
5-8 December 2016

Dynamics and Heat Transfer in Rotating Horizontal Convection at Large Rayleigh Number

C. A. Vreugdenhil[1], B. Gayen[1], and R. W. Griffiths[1]

[1]Research School of Earth Sciences
Australian National University, Australian Capital Territory 2601, Australia

Abstract

We examine the circulation forced by a gradient in surface temperature, known as horizontal convection, in a rectangular basin under planetary rotation. Direct numerical simulations are carried out to examine the problem in a closed rectangular basin that is heated over half of the base and cooled over the other half. Three Rayleigh numbers are considered, $Ra = 7.4 \times 10^8$, 7.4×10^{11} and 7.4×10^{12}, and Coriolis parameter is varied to give Ekman numbers in the range $E = 6.4 \times 10^{-8} - 1.6 \times 10^{-5}$. Other governing parameters are the Prandtl number $Pr = 5$ and vertical-to-length and horizontal-to-length aspect ratios, $A = 0.16$ and $C = 0.24$ respectively. The influence of rotation on flow dynamics and heat transfer depends on the natural Rossby number $Ro = U/fL = (E/Pr)(RaE)^{2/3}$ where U is the flow velocity in the thermal boundary layer that forms adjacent to the forced surface and f is the Coriolis parameter. When the system is in a rapidly rotation regime ($Ro < 0.1$) the flow is characterised by geostrophic balance in the thermal boundary layer. The heat transfer, expressed as a Nusselt number, decreases with rotation but increases with buoyancy forcing as $Nu \sim (RaE)^{1/3}$. A range of length scales are present in the rotating system that are associated with structures such as domain-scale gyres and full-depth convective vortices.

Introduction

A difference in temperature applied at the horizontal boundary of a fluid can generate a large-scale overturning circulation [7, 2]. This flow, known as horizontal convection, has application in the meridional overturning circulation of the oceans [8]. Rotation is expected to influence the horizontal convection flow by imposing a geostrophic balance which tends to inhibit flow in the direction of the temperature gradient and thereby decreases the net heat transfer through the system [6]. We examine the circulation forced by a gradient in surface temperature in a rectangular basin under planetary rotation, where the meridional sidewalls sustain boundary currents and domain-scale gyres.

A transition from laminar flow to turbulence has been identified in non-rotating horizontal convection [2]. For weaker buoyancy forcing ($Ra < 10^9$) the thermal boundary layer is laminar with flow governed by a viscous-buoyancy balance to produce Nusselt number (a measure of the dimensionless heat flux) that scales as $Nu \sim Ra^{1/5}$ where the Rayleigh number Ra is a measure of the strength of buoyancy forcing [7]. For stronger buoyancy forcing ($Ra > 10^{11}$) the boundary layer becomes convectively unstable and flow is dominated by an inertia-bouyancy balance with Nusselt number scaling as $Nu \sim (RaPr)^{1/5}$ where Pr is the Prandtl number [4, 2].

Scaling for the strong rotation geostrophic regime predicts a Nusselt number decreasing with increasing rotation as $Nu \sim (RaE)^{1/3}$ where E is the Ekman number [6, 5]. Laboratory experiments of a rotating rectangular box heated and cooled from below ($Ra \approx 10^{11}$) showed reasonable consistency with the geostrophic scaling for a limited range of rotation rates and Rayleigh numbers [5].

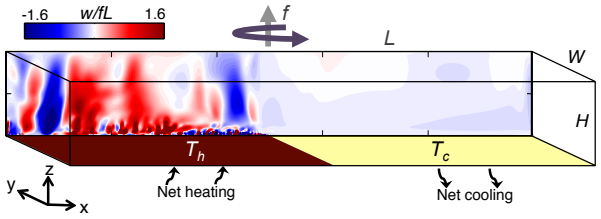

Figure 1. Setup of DNS solutions where half the base is heated and half is cooled. Inset is a snapshot of vertical velocity normalised by fL taken at $y/W = 0.91$ once the system had reached thermal steady state.

We use direct numerical simulations (DNS) to examine the dynamics and heat transfer of rotating horizontal convection in a rectangular box. Past simulations in a rotating re-entrant channel were at small Rayleigh number $Ra \sim O(10^9)$ [1]. We consider three Rayleigh numbers, with two large enough ($Ra > 10^{11}$) to correspond to a non-rotating case with a convectively unstable boundary layer. The maximum Ra is an order of magnitude larger than that previously reported [10]. A natural Rossby number compares the strength of the inertial term to the Coriolis term to collapse results across different Ra and allow further testing of the heat transfer geostrophic scaling.

Theory

We solve for the flow in a rectangular box of length L, width W and height H that is cooled to a uniform temperature T_c over half of the base and heated to a uniform temperature T_h over the other half (Figure 1). Governing parameters of rotating horizontal convection are the Rayleigh, Ekman and Prandtl numbers, and the vertical and horizontal aspect ratios, respectively

$$Ra = \frac{g\alpha\Delta T L^3}{\nu\kappa},\ E = \frac{\nu}{fL^2},\ Pr = \frac{\nu}{\kappa},\ A = \frac{H}{L},\ C = \frac{W}{L}, \quad (1)$$

where g is gravity, α is the coefficient of thermal expansion, $\Delta T = T_h - T_c$ is the imposed temperature difference, ν and κ are the molecular viscosity and diffusivity, and f is the (uniform) Coriolis parameter.

The governing equations are the Navier-Stokes momentum equation under the Boussinesq approximation with a linear equation of state, and the continuity of mass and heat, respectively

$$Pr^{-1}\left(\frac{D\hat{\mathbf{u}}}{D\hat{t}} + \nabla\hat{p}\right) = \nabla^2\hat{\mathbf{u}} + Ra\hat{T}\mathbf{k} - E^{-1}\mathbf{k}\times\hat{\mathbf{u}},$$

$$\nabla\cdot\hat{\mathbf{u}} = 0,\ \frac{D\hat{T}}{D\hat{t}} = \nabla^2\hat{T}, \quad (2)$$

where the bold font indicates vectors and the hats signify values non-dimensionalised by length L, mass $\rho_0 L^3$, time L^2/κ and temperature difference ΔT. Velocity vector is $\hat{\mathbf{u}} = (\hat{u}, \hat{v}, \hat{w})$, $\hat{t}$ is time, $\hat{p}$ is pressure deviation, $\hat{T} = (T - T_c)/\Delta T$ is temperature, and $\mathbf{k}$ is the unit upward vector.

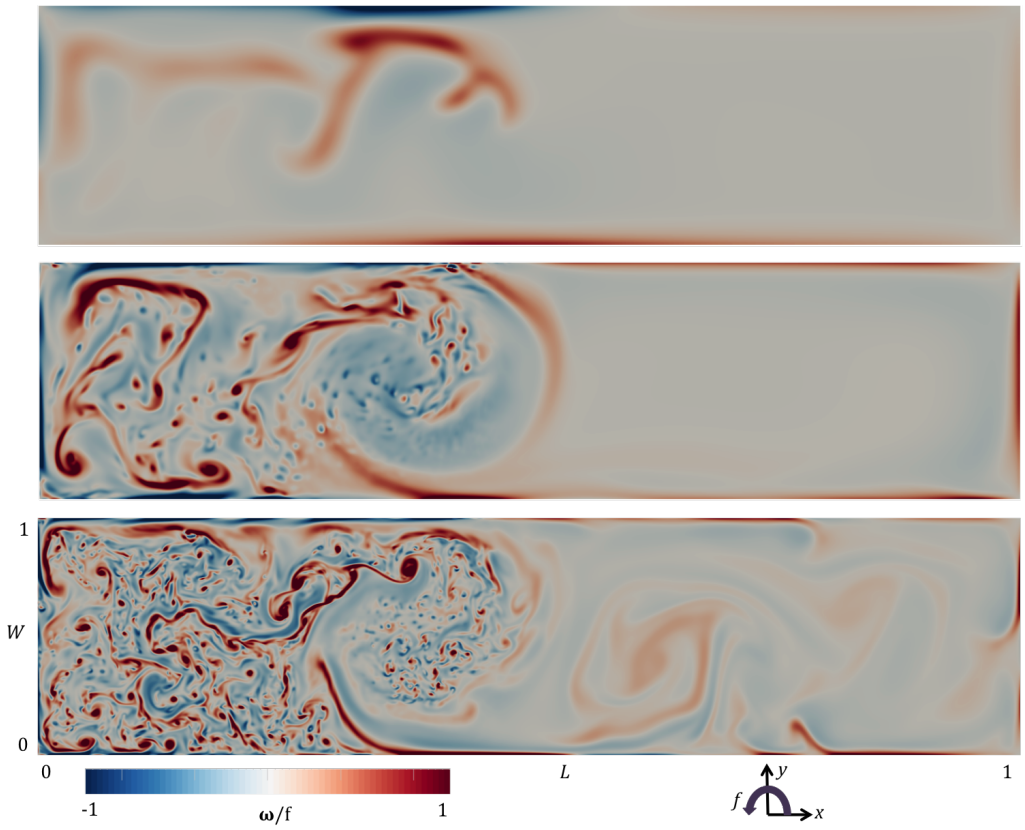

Figure 2. Vorticity snapshots taken within the thermal boundary layer at $z/H = 0.075$. (a) Upper: $Ra = 7.4 \times 10^8$, $E = 1.6 \times 10^{-5}$ ($Ro = 0.0017$); (b) middle: $Ra = 7.4 \times 10^{11}$, $E = 1.6 \times 10^{-6}$ ($Ro = 0.0036$); (c) lower: $Ra = 7.4 \times 10^{12}$, $E = 3.2 \times 10^{-7}$ ($Ro = 0.0011$). The vertical height of the planes as a fraction of thermal boundary layer thickness δ (measured as 90% of top-to-bottom density difference) for the three cases is (a) $z/\delta = 0.8$, (b) $z/\delta = 0.75$ and (c) $z/\delta = 1$. Vorticity values $\omega = \nabla \times u$ are normalised by f, rotation is anticlockwise and gravity is downward through the planes.

In the non-rotating regime with a laminar flow ($Ra < 10^9$) the thermal boundary layer is governed by a balance between the viscous and buoyancy terms [7] in the momentum equation (2). An assumption of an advection-diffusion balance over the cooled region of the boundary layer leads to the following scaling for velocity and Nusselt number,

$$U_{0v} \sim (\kappa/L)Ra^{2/5},\ Nu_{0v} = c_1 Ra^{1/5}, \tag{3}$$

where constant prefactor $c_1 = 0.37$ [2]. Nusselt number is defined as $Nu = FL/(\rho_0 c_p \kappa \Delta T)$ where F is the input heat flux per unit area, ρ_0 is the reference density and c_p is the specific heat. When the Rayleigh number is large enough ($Ra > 10^{11}$) the boundary layer is dominated by an inertial-buoyancy balance [4] and, coupled with the advection diffusion balance, gives

$$U_0 \sim (\kappa/L)(RaPr)^{2/5},\ Nu_0 = c_2(RaPr)^{1/5}, \tag{4}$$

where constant prefactor $c_2 = 0.37$ [2].

For the strong rotation regime, assuming horizontal velocities (u, v) within the thermal boundary layer scale similarly, a buoyancy-Coriolis balance becomes dominate in the momentum equation. Along with a balance of vertical advection and diffusion of heat within the boundary layer over the cooled region, this gives the geostrophic scaling

$$U \sim (\kappa/L)(RaE)^{2/3},\ Nu \sim (RaE)^{1/3}. \tag{5}$$

Defining the natural Rossby number as $Ro = U/fL = (E/Pr)(RaE)^{2/3}$ to write the Nusselt number scaling (5) normalised by the non-rotating large Ra scaling (4) as

$$Nu/Nu_0 = c_3 Ro^{1/5}, \tag{6}$$

where c_3 is a constant prefactor of $O(1)$ to be determined. Transition to the geostrophic regime occurs when $Ro < 0.1$. For the case coming from a non-rotating laminar regime, this is equivalent to the previously identified transition that the strongly rotating regime occurs when the Ekman layer thickness is thinner than the thermal boundary layer [3].

Model Setup

Direct numerical simulations solve the governing equations (2) for a closed rectangular box geometry (Figure 1). All boundaries are nonslip and all except the base are adiabatic. At the base a tanh temperature profile is imposed in the x-direction centred around $\hat{x} = 1/2$ to allow a smooth transition (of length $0.06L$) between the heated and cooled halves. The buoyancy $\alpha g \Delta T$ is varied to attain the three Rayleigh numbers ($Ra = 7.4 \times 10^8$, 7.4×10^{11} and 7.4×10^{12}). Other governing parameters are the Prandtl number $Pr = 5$, and vertical and horizontal aspect ratios, $A = 0.16$ and $C = 0.24$. The Coriolis parameter is varied to give Ekman numbers in the range $E = 6.4 \times 10^{-8} - 1.6 \times 10^{-5}$.

At larger Ra the smallest-scale structures in the flow (described by the Batchelor microscale $\eta_b = (\nu^3/\varepsilon)^{1/4} Pr^{-1/2}$ where ε is the local dissipation rate) are smaller and require higher grid resolution. To satisfy the resolution criterion for each grid cell, $\triangle_{x,y,z} \leq \pi\eta_b$, the solution grid for $Ra = 7.4 \times 10^{12}$ (1536 $\times$

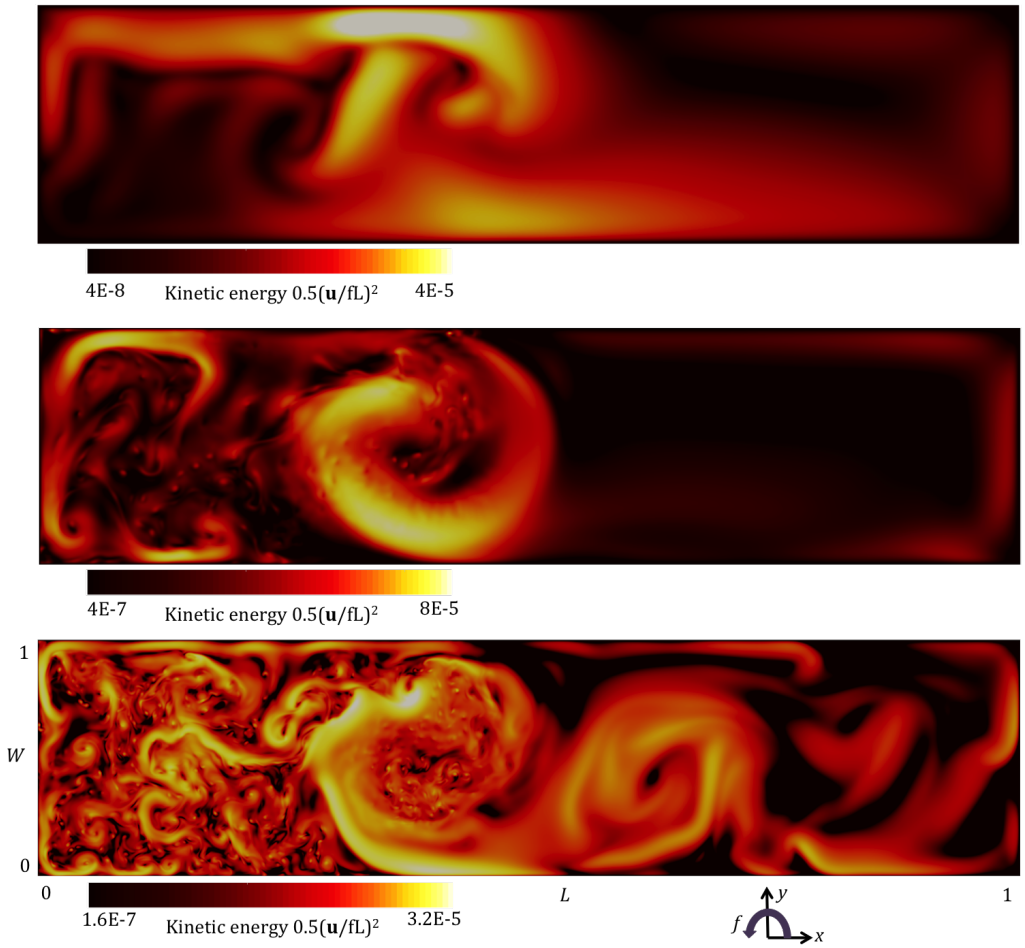

Figure 3. Kinetic energy snapshots taken within the thermal boundary layer at $z/H = 0.075$. (a) Upper: $Ra = 7.4 \times 10^8$, $E = 1.6 \times 10^{-5}$ ($Ro = 0.0017$); (b) middle: $Ra = 7.4 \times 10^{11}$, $E = 1.6 \times 10^{-6}$ ($Ro = 0.0036$); (c) lower: $Ra = 7.4 \times 10^{12}$, $E = 3.2 \times 10^{-7}$ ($Ro = 0.0011$). The vertical height of the planes as a fraction of thermal boundary layer thickness δ (measured as 90% of top-to-bottom density difference) for the three cases is (a) $z/\delta = 0.8$, (b) $z/\delta = 0.75$ and (c) $z/\delta = 1$. Kinetic energy values are normalised by $(fL)^2$, rotation is anticlockwise and gravity is downward through the planes.

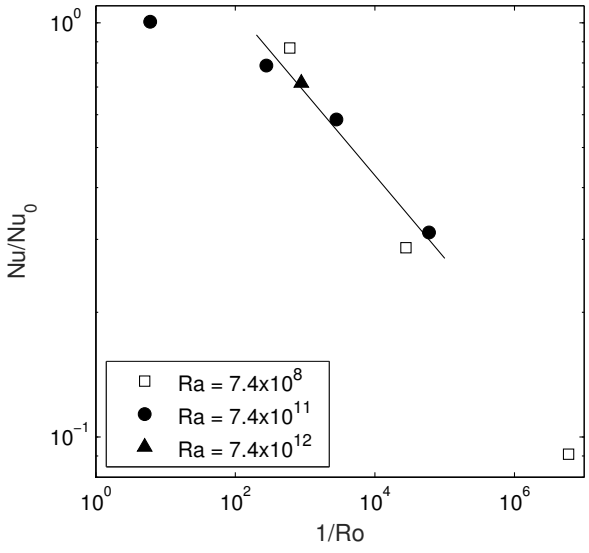

Figure 4. Nusselt number against the inverse Rossby number. Rotation rate increases along the horizontal axis. Geostrophic scaling (6) fitted to cases with $Ra > 10^{11}$ to give constant prefactor $c_3 = 2.7$.

512×512) contained more gird cells than for $Ra = 7.4 \times 10^{11}$ ($768 \times 256 \times 256$) or $Ra = 7.4 \times 10^{8}$ ($384 \times 128 \times 128$). The grid is clustered at the boundaries to resolve Ekman and Stewartson boundary layers. Accurate resolution was also confirmed by closure of the energy budget [2, 10]. As the largest *Ra* case was very computationally expensive, only one rotation ($E = 3.2 \times 10^{-7}$) was conducted at this *Ra*. All simulations were run until well after the thermal steady state was reached, where there is zero net heat flux through each horizontal level of the fluid in a time-averaged sense.

Results and Discussion

Dynamics

The strength of buoyancy forcing is an important influence on the range of scales present in the flow (Figures 2 and 3). For weaker buoyancy forcing ($Ra = 7.4 \times 10^{8}$; Figures 2a and 3a) the boundary layer is laminar with no sign of the small-scales of convection, consistent with the non-rotating laminar regime. The flow within the thermal boundary layer is dominated by concentrations of vorticity on each wall and an anticyclonic 'linear' region over the heated area.

As the buoyancy forcing is increased ($Ra = 7.4 \times 10^{11}$) a basin wide gyre forms over the heated region, and small-scale convective plumes appear as pin-pricks of positive relative vorticity (Figure 2b) and larger kinetic energy (Figure 3b). In the boundary layer over the cooled region a very weak cyclonic gyre forms and the time-average mean fields (not shown here) show another cyclonic gyre over the heated region near the endwall. The small-scale plumes can be drawn into convective vortices that appear as strong cyclonic spirals in the snapshot fields, and these vortices can penetrate through the boundary layer stratification into the interior and indeed through the full-depth. Snapshots of vertical velocity such as that shown in Figure 1 (inset) show the small-scale convection in the boundary layer, along with evidence of cyclonic vortices throughout the depth outside the boundary layer over the heated region. Motion over the cooled region is quite slow and of relatively large scale.

At the strongest buoyancy forcing ($Ra = 7.4 \times 10^{12}$; Figures 2c and 3c) the boundary layer flow contains a broader range of length scales. The convective plumes become smaller in size and many more form across the heat region, which become a 'sea' of convective vortices that penetrate into the interior. A large anticyclonic gyre over the heated end is clear in the snapshot planes, similar in placement and size to the anticyclonic gyre noted for $Ra = 7.4 \times 10^{11}$. Over the cooled region there is notable circulation in the boundary layer with evidence of a cyclonic gyre and the mean fields (not shown here) show large-scale cyclonic motion over the remaining heated region.

Heat transfer

We define the dimensionless heat transport, or Nusselt number, as $Nu = |\overline{dT/dz}|/(\Delta T/L)$ where $\overline{dT/dz}$ is the vertical temperature gradient at the bottom boundary $z = 0$ horizontally averaged over the cooled region. The resulting *Nu* was then time-averaged over many buoyancy timescales to average out any unsteadiness in the flow.

The Nusselt number is consistent with the geostrophic scaling once $Ro < 0.1$ and decreases with increasing rotation rate (Figure 4). By plotting *Nu* against *Ro* the results for different *Ra* collapse, although we note that as the Nusselt number axis has been non-dimensionalised by the non-rotating case, the geostrophic scaling for $Ra = 7.4 \times 10^{8}$ (not shown here) is predicted to be slightly offset by a factor of $Pr^{1/5}$ due to differences in the non-rotating scaling for the laminar (3) and inertial (4) regimes. The experiment at $Ra = 7.4 \times 10^{8}$ and very small *Ro* is thought to be in an extreme rotation regime, where rotation is so strong that advection is largely shut down and heat transport is primarily via conduction. This conduction regime was also reported for simulations of axisymmetric rotating horizontal convection [9].

Conclusions

Large-scale gyres are present when rotation is strong enough to place the flow in the geostrophic regime, buoyancy forcing ($Ra > 10^{11}$) is required to produce small-scale convection and rotationally induced full-depth convective vortices. The Nusselt number is smaller for larger rotation consistent with scaling based on geostrophic balance within the thermal boundary layer. The heat transport from the heated boundary layer into the interior (where it is then carried to the cooled end) is not via an endwall plume, as in the non-rotating case, but via many small vortical plumes that are widely distributed over the heated region. This is reminiscent of 'open ocean' deep convection, which similarly involves broad areas (chimneys) of vertical convection consisting of a field of small (1 km) scale plumes.

Acknowledgements

The research was supported by the Australian Research Council (ARC) grant DP140103706 and BG was funded by an ARC ECR DE140100089. Numerical computations were carried out on the Australian National Computational Infrastructure, ANU.

References

[1] Barkan, R., K. B. Winters, and S. G. Llewellyn Smith, Rotating horizontal convection, *J. Fluid Mech.*, **723**, 2013, 556–586.

[2] Gayen, B., Griffiths, R. W., and Hughes, G. O., Stability transitions and turbulence in horizontal convection, *J. Fluid Mech.*, **751**, 2014, 698–724.

[3] Hignett, P., A. Ibbetson, and P. D. Killworth, On rotating thermal convection driven by non-uniform heating from below, *J. Fluid Mech.*, **109**, 1981, 161–187.

[4] Hughes, G. O., R. W. Griffiths, J. C. Mullarney, and W. H. Peterson, A theoretical model for horizontal convection at high Rayleigh number, *J. Fluid Mech.*, **581**, 2007, 251–276.

[5] Park, Y.-G., and J. A. Whitehead, Rotating Convection Driven by Differential Bottom Heating, *J. Phys. Oceanogr.*, **29**, 1999, 1208–1220.

[6] Robinson, A., and H. Stommel (1959), The Oceanic Thermocline and the Associated Thermohaline Circulation, *Tellus*, **11**, 295–308.

[7] Rossby, H. T. (1965), On thermal convection driven by non-uniform heating from below: an experimental study., *Deep-Sea Res.*, **12**, 9–16.

[8] Saenz, J. A., A. M. Hogg, G. O. Hughes, and R. W. Griffiths, Mechanical power input from buoyancy and wind to the circulation in an ocean model, *Geophys. Res. Lett.*, **39**, 2012, L13605.

[9] Sheard, G. J., W. K. Hussam, and T. Tsai, Linear stability and energetics of rotating radial horizontal convection, *J. Fluid Mech.*, **795**, 2016, 1–35.

[10] Vreugdenhil, C. A., B. Gayen, and R. W. Griffiths, Mixing and dissipation in a geostrophic buoyancy-driven circulation, *J. Geophys. Res.*, accepted, 2016.